Prediction of the Nonlinear Aerodynamic Characteristics of Maneuvering Missiles

Michael R. Mendenhall,* Stanley C. Perkins Jr.,† and Daniel J. Lesieutre†
Nielsen Engineering & Research, Inc., Mountain View, California

An analytical method to predict the nonlinear aerodynamic forces and moments on a missile undergoing steady and unsteady maneuvers is described. The major physical flow phenomena over the missile are simulated, including the leeside separation vorticity. The mutual interaction between the vehicle and the time-dependent flowfield is considered in the prediction of the unsteady aerodynamic characteristics at any specified instant in time. The aerodynamic prediction method is coupled with a solver of the six-degree-of-freedom equations of motion to predict missile trajectories or it is used for models undergoing forced trajectories or oscillating motions. The prediction method is verified by comparison with experimental data where possible. Flowfields near a missile in oscillating motion are compared with flow visualization photographs.

Nomenclature

c_n = normal force coefficient per unit length
C_p = pressure coefficient
C_m = pitching moment coefficient
C_N = normal force coefficient
d = diameter
f = pitching frequency
i,j,k = unit vectors in x,y,z system
I = moment of inertia
k = reduced frequency, $\pi fd/V_\infty$
ℓ = missile length
m = mass
M' = pitching moment
p = rolling rate and local static pressure
p_∞ = static pressure
q = pitching rate
q_∞ = freestream dynamic pressure, $\rho V_\infty^2/2$
q' = nondimensional pitching rate, $q\ell/V_\infty$
r = yawing rate
r_0 = missile radius
R = radial distance
Re = Reynolds number
t = time
u_e = crossflow velocity at boundary-layer edge, Eq. (1)
V_∞ = freestream velocity
u,v,w, = perturbation velocities
W = weight
$W(\sigma)$ = complex velocity potential
x,y,z = missile coordinate system, origin at center of gravity
x_i,y_i,z_i, = inertial coordinate system
X,Y,Z = missile coordinate system, origin at nose
Z' = normal force
α = angle of attack
α' = local angle of attack
α_c = angle between freestream velocity vector and body axis
β = angle of yaw
β' = local angle of yaw
Γ = vortex strength
Δt = time increment
ΔX = axial length increment
θ = polar angle, Fig. 2
ρ = freestream density
σ = complex coordinate
ϕ = roll angle and velocity potential
Φ = velocity potential
ψ = stream function
ω = rotation rate

Subscripts

$(\bar{\ })$ = conjugate of complex quantity
AM = apparent mass
B = body
P = point P on missile
s = steady
u = unsteady

Introduction

OPERATIONAL requirements of modern flight vehicles, both aircraft and missiles, can involve dynamic maneuvers that result in very high angles of incidence and large angular rates. Under such flow conditions, the vehicle experiences important nonlinear aerodynamic forces and moments due to flow separation and roll up of the leeside vortices (Fig. 1). In unsteady flow, the strength and position of these vortices and their induced effects are dependent on the history of the motion of the vehicle and, conversely, the motion of the vehicle is dependent on the vortex-induced aerodynamic effects. Prediction of the vehicle motion when the aerodynamic characteristics are dominated by high-angle nonlinear effects requires a different approach from traditional linear prediction methods which are applicable to low-angle unseparated flow conditions. Unsteady nonlinear techniques are required for predicting and understanding the complex flow phenomena involved in high-angle maneuvers.

An engineering prediction method to simulate the major physical features of the flow around a body of revolution undergoing steady or unsteady motions in incompressible flow is described in this paper. The aerodynamic prediction method is coupled to a solver of the six-degree-of-freedom equations of motion for direct calculation of missile trajectories without

Presented as Paper 85-1776 at the AIAA Atmospheric Flight Mechanics Conference, Snowmass, CO, Aug. 19-21, 1985; received Sept. 16, 1985; revision submitted Aug. 14, 1986.

*Vice President and Principal Engineer. Associate Fellow AIAA.
†Research Engineer. Member AIAA.

the need for the complete set of stability derivatives or large quantities of empirical information.

The genesis of the aerodynamic method described herein is the discrete vortex cloud model of the leeside vorticity shed from bodies at high angles of attack.[1-3] This nonlinear flow model for prediction of static aerodynamic characteristics was extended to handle configurations undergoing steady flow with constant incidence angles and constant angular rotation rates in Ref. 4. Such a flow condition is achieved when a body is moving along a circular-arc path while inclined at a constant angle to the path. The steady flow model was further extended to include unsteady motion in Ref. 5.

The purpose of this paper is to describe both the extension of the vortex cloud method to unsteady flows and the vehicle trajectory analysis. The following sections include a discussion of the approach to the problem and a description of the analysis and flow models required to carry out the calculations. Where possible, the prediction method is evaluated through comparison of measured and predicted results for a variety of flow conditions.

General Approach

The engineering prediction method described herein is applicable to flight vehicles maneuvering at high angles of incidence in a flow regime in which the aerodynamic characteristics are dominated by nonlinear effects. The prediction method represents the complex physical phenomena in the flowfield adjacent to the vehicle, including both steady and unsteady hull separation vorticity and lifting surface trailing vorticity. Vehicles can have a wide range of configurations and component arrangements, but for purposes of this discussion, the flow model is directed at axisymmetric bodies with fore and/or aft lifting surfaces.

The major nonlinear effect on a missile at high angles of incidence in both steady and unsteady flow conditions is the separation vortex wake on the leeside of the body. The vorticity is formed by boundary-layer fluid leaving the body surface from separation points on both sides of the missile. The vorticity rolls up into a symmetrical vortex pair (Fig. 1). These vortices induce nonlinear effects that can dominate the aerodynamic forces and moments and thus can have a major influence on the missile trajectory. A successful approach to modeling the leeside vorticity under static flow conditions is the representation of the vortex wake by a cloud of discrete vortices. As described by the present authors[1-3] and other investigators,[6-8] the vortex cloud model is a reasonable means to predict the induced effect of a very complex flow phenomenon. The selected approach to the more complex problem of maneuvering missiles will begin with the basic vortex cloud model and extend it to the more complicated unsteady flows.

Details of the flow models and the calculation procedures are described in the following sections.

Methods of Analysis

Much of the analysis for the prediction method developed in this investigation is available in referenced sources, but parts of the unsteady analysis are not readily available. The following sections will discuss only briefly the previously published information; the unpublished analyses will be presented in more detail as space permits.

Geometry

A three-dimensional singularity distribution is required for calculating velocities at any point in the flowfield outside the body surface and for calculating the surface pressure distribution on the surface. The fuselage is defined as a body of revolution without appendages and the volume effects are represented by a series of point sources and sinks distributed on the axis. This type of three-dimensional representation is described in Refs. 3 and 9 for missile shapes. Briefly, the sources and sinks are distributed on the body axis with an optimum spacing determined by the radius distribution of the body. The strengths of the individual singularities are determined from the solution of specific boundary conditions (including the body radius and slope at a number of stations along the body), a stagnation point on the nose, and the requirement of a closed body.

Although not presented in this discussion, the flow model also includes two regions on the body containing multiple lifting surfaces. Each fin or lifting surface is represented by a lattice of horseshoe vortices, the strengths of which are obtained by satisfying the flow tangency condition on the fin. This provides a trailing vortex field, which is included with the vortex field associated with separation from the body.

Discrete Vortex Model

The derivation of the discrete vortex model of the leeside wake on a missile at high angles of incidence is discussed in detail in Refs. 1-3. A brief outline of the method follows.

At a specified angle of attack, the pressure distribution near the nose is calculated in a crossflow plane normal to the missile axis. The pressure distribution is examined for separation using the Stratford laminar[10] or turbulent[11] separation criteria, the choice depending on the Reynolds number. If separation is indicated, a discrete two-dimensional vortex is shed into the flow from the separation point. The strength of the vortex is

$$\frac{\Gamma}{V_\infty} = \frac{u_e^2}{2V_\infty^2} \frac{\Delta X}{\cos\alpha_c} \delta \tag{1}$$

where δ is an empirical vortex reduction factor.[3,6] Equation (1) is obtained by integration across the boundary layer, assuming no slip at the wall. The initial position of the shed vortex is determined such that the surface velocity in the crossflow plane at the separation point is exactly canceled by the shed vortex and its image. From this moment, the vortex becomes free and is permitted to move with the local flowfield under the effects of the freestream, the missile, and other vortices.

The equations of motion of each vortex in the field are integrated over the distance between the crossflow plane in which they were shed and the next crossflow plane on the missile (ΔX). At the next crossflow plane, the pressure distribution is predicted, this time including the influence of the vortices in the flowfield. As before, the predicted pressure distribution is tested for separation and, if indicated, additional vortices are shed into the field adding to the wake. The marching procedure continues to the base of the missile. Since the pressure distribution on the missile is known, the forces and moments are obtained by integration over the missile surface.

Steady Motion

The static analysis was extended to a simple case of steady motion defined as the missile moving with constant α, β, p,

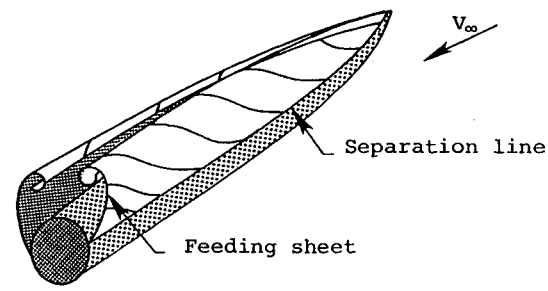

Fig. 1 Leeside vortex formation.

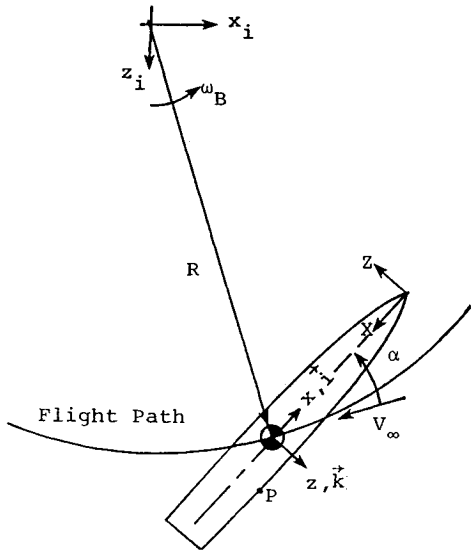

a) Pitch plane nomenclature.

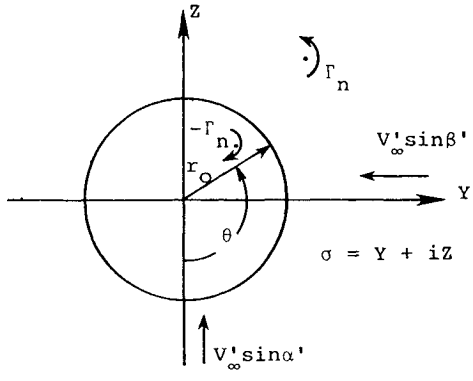

b) Crossflow plane nomenclature.

Fig. 2 Missile coordinate system for steady flow.

q, and r motions. An example of this type of motion is a missile moving in a steady turn at constant angles and rates and it is represented experimentally by moving the missile on a circular-arc path with a constant inclination angle to the path. Practically, this is accomplished by attaching the missile to a rotating arm apparatus at a fixed angle of incidence (Fig. 2). Even though a typical experiment may involve motion in one plane (that is, motion with constant α and q or constant β and r), the analysis considers arbitrary motion with constant angles and rotation rates.

The calculation of the aerodynamic characteristics is carried out with a marching procedure in the same manner as the static approach. The basic discrete vortex shedding model is unchanged; however, the surface pressure calculation and the vortex tracking procedures reflect the fact that the missile is in steady flow that is changing along the body. The strength and position of the vortex wake and its induced effect on the missile become a function of the motion of the missile.

Pressure Coefficient

The relationship for the pressure on a moving body is[12]

$$\frac{p}{\rho}+\frac{1}{2}q_r^2+\frac{\partial\Phi}{\partial t}-\frac{1}{2}V^2=\frac{p_\infty}{\rho} \tag{2}$$

with respect to the moving reference frame fixed in the body (Fig. 2). In Eq. (2), q_r is the fluid velocity at a point P fixed relative to the body-fixed or moving axis system and V the speed of point P in the inertial axis system.

The components of the fluid velocity at point P in the x,y,z system are:

Due to body motion,

$$V_\infty=-V_\infty\cos\alpha_c i-V_\infty\sin\beta j-V_\infty\sin\alpha k \tag{3}$$

due to body rotation,

$$\omega\times R_p=(ry-qz)i-(pz-rx)j+(qx-py)k \tag{4}$$

and due to perturbation velocities,

$$V'=ui+vj+wk \tag{5}$$

The angles of attack and yaw are

$$\sin\alpha=\sin\alpha_c\cos\phi$$

$$\sin\beta=\sin\alpha_c\sin\phi \tag{6}$$

where α_c and ϕ are angles specified in steady flow and calculated in unsteady flow.

The perturbation velocities in Eq. (5) consist of induced velocity components due to body-volume effects, shed vortices, and fins on the body if present. From Eqs. (3-5), the fluid velocity at point P is

$$q_r=V'+V_\infty+(\omega\times R_p) \tag{7}$$

and the velocity of point P with respect to the inertial reference frame is

$$V=V_{\infty_B}+(\omega_B\times R_p) \tag{8}$$

where V_{∞_B} is equal in magnitude and opposite in direction to V_∞ from Eq. (3).

Since a steady-flow condition is assumed for this analysis, the unsteady term in Eq. (2) disappears because this pressure relation is for the complete missile and Φ is the full three-dimensional velocity potential. When the details of calculating the pressure distribution are considered and both two- and three-dimensional singularities are involved, a similar term reappears in the pressure equation. This term, involving $d\Phi/dx$, is described in Refs. 1 and 2 and is discussed later in this section.

Defining the pressure coefficient as

$$C_p=\frac{p-p_\infty}{\frac{1}{2}\rho V_\infty^2} \tag{9}$$

Eq. (2) becomes

$$C_p=-\left[\left(\frac{u}{V_\infty}\right)^2-2\left(\frac{u}{V_\infty}\right)\cos\alpha_c-2\left(\frac{u}{V_\infty}\right)\left(\frac{qz}{V_\infty}-\frac{ry}{V_\infty}\right)+\left(\frac{v}{V_\infty}\right)^2-2\left(\frac{v}{V_\infty}\right)\sin\beta-2\left(\frac{v}{V_\infty}\right)\left(\frac{rx}{V_\infty}-\frac{pz}{V_\infty}\right)+\left(\frac{w}{V_\infty}\right)^2-2\left(\frac{w}{V_\infty}\right)\sin\alpha-2\left(\frac{w}{V_\infty}\right)\left(\frac{py}{V_\infty}-\frac{qx}{V_\infty}\right)\right] \tag{10}$$

where u, v, and w are perturbation velocities associated with body-volume effects and shed vorticity.

Certain aspects of the calculation procedure involving the two-dimensional singularities make it advantageous to transform to the X,Y,Z coordinate system with its origin at the nose of the missile (Fig. 2). The above analysis is easily changed to the new system and, in the remainder of this paper, the equations are referred to this body-fixed system.

Based on the use of both two- and three-dimensional singularities, the pressure relation is

$$C_{p_s}=\frac{p-p_\infty}{\frac{1}{2}\rho V_\infty^2}-\frac{2\cos\alpha_c}{V_\infty}\frac{d\phi}{dX} \tag{11}$$

where ϕ is the two-dimensional velocity potential in crossflow planes of the missile. This term, in effect, represents the u-perturbation velocities associated with the two-dimensional singularities used in the flow model. For example, the doublet terms and the discrete vortices in each crossflow plane contribute to this term, which is unsteady in the axial coordinate X but steady in time. Finally, the pressure coefficient on a missile undergoing steady translational and rotational motion is

$$\begin{aligned}C_p=-\Big\{&\left(\frac{u}{V_\infty}\right)^2+2\left(\frac{u}{V_\infty}\right)\cos\alpha_c-2\left(\frac{u}{V_\infty}\right)\left(\frac{qZ}{V_\infty}+\frac{rY}{V_\infty}\right)\\&+\left(\frac{v}{V_\infty}\right)^2-2\left(\frac{v}{V_\infty}\right)\sin\beta-2\left(\frac{v}{V_\infty}\right)\left[\frac{pZ}{V_\infty}+\frac{r}{V_\infty}(X_{CG}-X)\right]\\&+\left(\frac{w}{V_\infty}\right)^2+2\left(\frac{w}{V_\infty}\right)\sin\alpha-2\left(\frac{w}{V_\infty}\right)\left[\frac{q}{V_\infty}(X_{CG}-X)-\frac{pY}{V_\infty}\right]\Big\}\\&-\frac{2\cos\alpha_c}{V_\infty}\frac{d\phi}{dX}\end{aligned} \tag{12}$$

The derivation of the last term is described in the next section.

Velocity Field

Velocity components are required for prediction of the missile surface pressure distribution and for vortex trajectory calculations. These components originate from both two- and three-dimensional flow models. Since the two-dimensional velocity potential is needed for the unsteady term in the pressure equations, it will be considered in detail.

Referring to Fig. 2, each crossflow plane on the missile has associated with it a complex two-dimensional potential,

$$W(\sigma)=\phi+i\psi \tag{13}$$

where the complex coordinate is

$$\sigma=Y+iZ \tag{14}$$

Components of the complex potential are as follows. Crossflow due to uniform α and β is

$$W_1(\sigma)=-i\sigma V_\infty\sin\alpha \tag{15}$$

$$W_2(\sigma)=-\sigma V_\infty\sin\beta \tag{16}$$

where $\sin\alpha$ and $\sin\beta$ are defined in Eq. (6). Note that terms associated with the rotation of the missile are not included in Eqs. (15) and (16). These are not strictly two-dimensional terms and they are included with the three-dimensional velocity components.

The doublet terms representing a cylinder in α' and β' flow are

$$W_3(\sigma)=i(r_0^2/\sigma)V_\infty'\sin\alpha' \tag{17}$$

$$W_4(\sigma)=-(r_0^2/\sigma)V_\infty'\sin\beta' \tag{18}$$

where the equivalent local angles of incidence including effects of rotation-induced velocities are

$$\sin\alpha'=\frac{V_\infty\sin\alpha+w_q}{V_\infty'} \tag{19}$$

$$\sin\beta'=\frac{V_\infty\sin\beta+v_r}{V_\infty'} \tag{20}$$

The rotation-induced velocities are included in the doublet terms because they have a direct effect on the strength of these two-dimensional singularities.

The total freestream velocity as defined in the crossflow plane is

$$(V_\infty')^2=(V_\infty\cos\alpha_c)^2+(V_\infty\sin\beta+v_r)^2+(V_\infty\sin\alpha+w_q)^2 \tag{21}$$

where

$$w_q=-(X_{CG}-X)q \tag{22}$$

$$v_r=(X_{CG}-X)r \tag{23}$$

The velocity potentials due to the discrete vortices and their images are

$$W_5(\sigma)=-i\sum_{n=1}^{N}\frac{\Gamma_n}{2\pi}\ell n(\sigma-\sigma_n) \tag{24}$$

$$W_6(\sigma)=i\sum_{n=1}^{N}\frac{\Gamma_n}{2\pi}\ell n\left(\sigma-\frac{r_0^2}{\bar{\sigma}_n}\right) \tag{25}$$

The "unsteady" two-dimensional term in the pressure equation (12) is evaluated on the missile surface as

$$\frac{d\phi}{dX}=\text{Real}\left.\frac{dW(\sigma)}{dX}\right|_{r=r_0} \tag{26}$$

where the required complex potential is

$$\begin{aligned}W(\sigma)&=\phi+i\psi\\&=\frac{r_0^2}{\sigma}V_\infty'(-\sin\beta'+i\sin\alpha')\\&\quad+\sum_{n+1}^{N}\frac{\Gamma_n}{2\pi}\left[-i\ell n(\sigma-\sigma_n)+i\ell n\left(\sigma-\frac{r_0^2}{\bar{\sigma}_n}\right)\right]\end{aligned} \tag{27}$$

Note that the uniform flow terms are not included since they do not contribute to the unsteady pressure term.

The total two-dimensional complex potential is given by the sum of Eqs. (15-18), (24), and (25). The two-dimensional velocity components in the crossflow plane are obtained from

$$\frac{dW(\sigma)}{d\sigma}=v-iw \tag{28}$$

Details of the character of the individual velocity components are presented in Ref. 3. To these components must be added the u, v, and w velocity components from the rotation of the missile and the three-dimensional source and sink distribution representing the body-volume effects.

Unsteady Motion

The unsteady aerodynamic analysis of a missile undergoing time-dependent maneuvers involving large incidence angles and angular rates begins with the steady analysis in the preceeding section. The initial conditions for an unsteady maneuver are the steady-flow conditions used to develop initial forces and moments and a leeside vortex wake.

Predicted forces and moments on the missile are used to calculate the motion of the missile over a small time interval, assuming the forces and moments and flow conditions are constant over the interval. The trajectory calculation produces new flow conditions and time rates of change of flow variables at the end of the interval. The vortex wake is al-

lowed to move downstream under the influence of the changing local flow conditions during the interval Δt where it influences the pressure distribution and subsequent separation. New vortices are added to the field, new forces and moments are computed, and the calculation procedure is repeated. The vortex wake represents the historical lag in the flowfield, which relates to the aft portion of the vehicle what happened at an earlier time on the nose. The early portions of the wake are eventually swept downstream past the base of the body and their effect on the induced loads is lost forever.

Pressure Coefficient

Starting with the relationship for the pressure on a moving body [Eq. (2)], the unsteady pressure equation is developed in a parallel manner to the previous analysis, except that the total velocity potential Φ is changing with time. The unsteady pressure coefficient is

$$C_{p_u} = C_{p_s} - \frac{2}{V_\infty^2}\frac{\partial \Phi}{\partial t} \tag{29}$$

where C_{p_s} is the instantaneous steady pressure coefficient from Eq. (12).

Each two- and three-dimensional singularity of the flow model is changing with time and contributes to the unsteady pressure term as long as the velocity potential satisfies the condition that it be equal to zero or constant at infinity in the inertial reference frame. The major three-dimensional singularity distribution is the source-sink model of the body. Since the missile shape is not changing with time, the time-dependent variables are the freestream velocity and the incidence angle; therefore, this term is considered analytically. The two-dimensional velocity potentials are described above. The derivatives with time can be accomplished analytically for all but the terms associated with the wake vorticity. Because of the discrete vortex formulation of the wake and the numerical integration procedure used in the wake trajectory calculation, a simple differencing technique is applied to evaluate the unsteady terms representing the vortex wake.

Flow Model

The basic flow model used for the unsteady analysis is virtually identical to that developed for steady-flow conditions. This obviously involves certain assumptions. For example, it is assumed that a mix of two- and three-dimensional singularities is appropriate for an engineering prediction method in unsteady flow.

A more basic question, which cannot be resolved with empirical information at this time, is the use of static, flat-plate, separation criteria in a time-dependent flowfield. This approximation may well be the weakest link in the prediction method, even though it has proved successful in both static and steady flows.

Development of the discrete vortex cloud in unsteady flow requires a unique application of the vortex tracking procedures used in static and steady flow. As previously mentioned, the initial separation characteristics and shed vorticity field are determined for a steady flow condition at $t_0 = 0$. A sketch of the resulting flowfield is shown in Fig. 3. For purposes of this discussion, the missile is divided into axial increments, each of length ΔX. The discrete vortex positions are shown as dots at each X station and the individual paths are denoted by dashed lines between X stations. Individual vortices are identified as $\Gamma_{m,t}$, where the first subscript represents the axial station at which they are shed and the second represents the time step.

The time interval for each step of a trajectory calculation is specified by the axial spacing ΔX chosen for the vortex wake calculation. That is,

$$\Delta t \leq (\Delta X / V_\infty \cos\alpha_c) \tag{30}$$

where V_∞ and α_c are average values between time steps. The above interval was chosen to provide sufficient time for the changing vortex effects to influence the calculation before being swept past the base of the missile. Typically, ΔX is approximately equal to the maximum radius of the missile.

Given new flow conditions at t_1, the vortex wake from $t_0 = 0$ is allowed to move downstream under the influence of modified local flow conditions during the interval Δt. The average conditions at $\Delta t/2$ are considered appropriate for the entire interval. A new vortex field is shown in Fig. 3b. Comparison of Figs. 3a and 3b illustrates how the individual vortices making up the cloud move in the axial direction. The entire vortex field shed at t_0 has been transported downstream a distance ΔX. Now, under the influence of the actual flow conditions at t_1 and the modified vortex field, the body pressure distribution is predicted and a new separation calculation is made. The situation at t_1 is shown in Fig. 3c, where the new vortices at each station are shown added to the total field. The calculation procedure is repeated at $t_2 = t_1 + \Delta t$ and so on.

The moving vortex wake relates to the base of the missile what happened at an earlier time on the nose of the missile. As the calculation progresses, the wake shed at an earlier time is swept downstream past the base and the effect on the missile is lost forever. For practical considerations, the vortex wake is continued one or two diameters beyond the base of a missile with tail fins.

Trajectory Analysis

A common approach to the prediciton of missile trajectories involves the integration of the six-degree-of-freedom equations of motion of the missile over the time frame of interest. The standard equations of motion are written in a form that requires the stability derivatives for the configuration of interest for the range of flow conditions to be considered.[13] This creates difficulties when the stability derivatives are unknown, either because the configuration is unusual or of a preliminary nature, or because the flight regime involves nonlinear aspects that make it impossible to determine the derivatives experimentally. The following analysis is an attempt to circumvent these problems.

In the current investigation, the equations of motion are written without individual stability derivatives. Instead, the equations are written in terms of the forces and moments and the solution relies on the direct calculation of the missile forces and moments at any instant in time. Only the normal force and pitching moment equations are presented below; however, the equations for the other planes are developed in

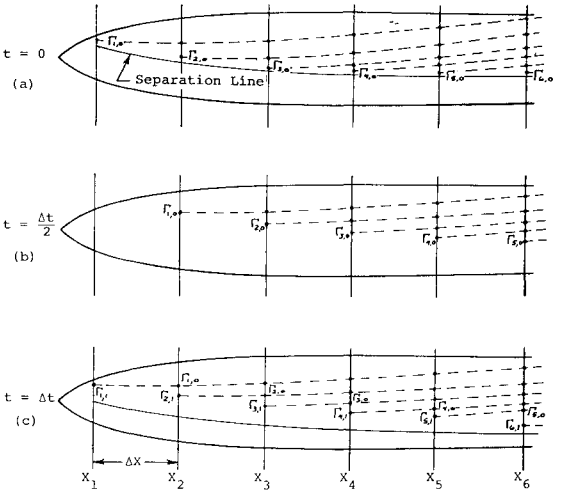

Fig. 3 Unsteady vortex tracking procedure.

a similar manner, as

Normal force:

$$(m-C_5)\dot{w}-C_6\dot{q}=m(uq-vp)+(Z'-Z'_{AM})+W\cos\theta\cos\phi \tag{31}$$

Pitching moment:

$$(I_{yy}-C_{10})\dot{q}-I_{xy}\dot{p}-I_{yz}\dot{r}-C_{11}\dot{w}=(I_{zz}-I_{xx})rp+(M'-M'_{AM}) \tag{32}$$

The equations are based on a configuration with its origin at the center of gravity and with the positive senses of forces and moments, velocities, and angular rates indicated in Fig. 4. The angles ϕ, θ, and ψ in Eqs. (31) and (32) are the Euler angles relating the orientation of the body-fixed coordinate system to the inertial system. The C_i coefficients and the subscript AM are added-mass terms. These terms have been removed from the right-hand side of the above equations to eliminate the numerical instability in the solution, as discussed in Ref. 14.

A trajectory calculation is carried out in the following manner. Starting with initial flow conditions and the missile orientation in the inertial coordinate system, a steady flow solution is obtained to provide a vortex wake and the forces and moments with which to begin the unsteady calculation. The unsteady calculation begins with the prediction of the missile motion from $t_0=0$ to $t_1=\Delta t$, where Δt is given in Eq. (30). It is assumed for this preliminary analysis that the flow conditions and missile loads are constant over the Δt interval. The six-degree-of-freedom equations of motion are solved to determine new velocity components, angular rates, coordinates of the missile center of gravity (c.g.), and orientation of the missile at t_1.

The vortex wake is permitted to move in the time interval to its new position as described in a previous section. With the new wake position and the modified flow conditions at t_1, the forces and moments on the missile are computed. This process continues to the end of the specified trajectory calculation.

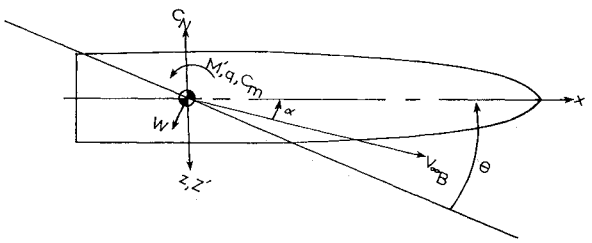

Fig. 4 Pitch plane coordinate system for unsteady motion.

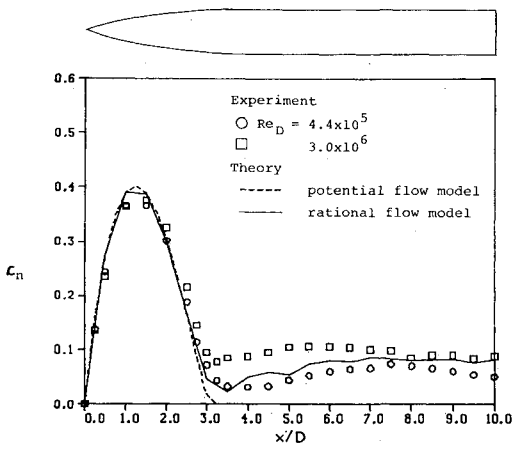

Fig. 5 Measured and predicted normal force distribution on an oglive-cylinder missile, $\alpha=15$ deg.

Results

The ultimate evaluation of the applicability of the engineering prediction method proposed in this paper is through comparisons of measured and predicted aerodynamic characteristics on a variety of missile configurations under a wide range of flight conditions. Unfortunately, little experimental data other than static aerodynamic characteristics are available. In this section, static results are presented to verify the applicability of the discrete vortex approach further, some steady turning results are discussed to illustrate effects of turn rate, and an unsteady maneuver is shown to demonstrate the method.

Static Characteristics

The method was applied to a missile configuration consisting of a 3-caliber ogive nose and a 7.7-caliber cylindrical afterbody.[15] For purposes of this discussion, all comparisons shown are for $\alpha=15$ deg; however, the entire angle-of-attack range was investigated and these results are considered typical.

Measured and predicted axial distributions of normal forces are compared in Fig. 5. The agreement is good over most of the missile length; however, near the base, the predicted results appear to agree better with measurements for the high Reynolds number than those for the lower. The predicted results for no separation, which correspond to potential flow, are shown as a dashed curve.

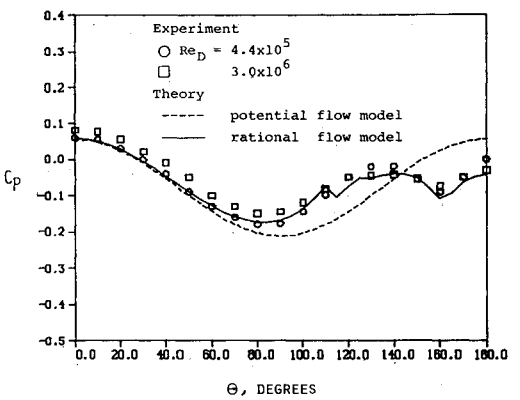

Fig. 6 Measured and predicted pressure distribution on an ogive-cylinder missile, $X/D=7.5$, $\alpha=15$ deg.

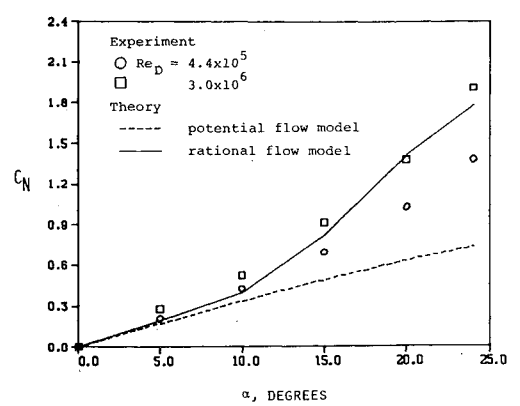

Fig. 7 Measured and predicted normal force coefficient on an ogive-cylinder missile.

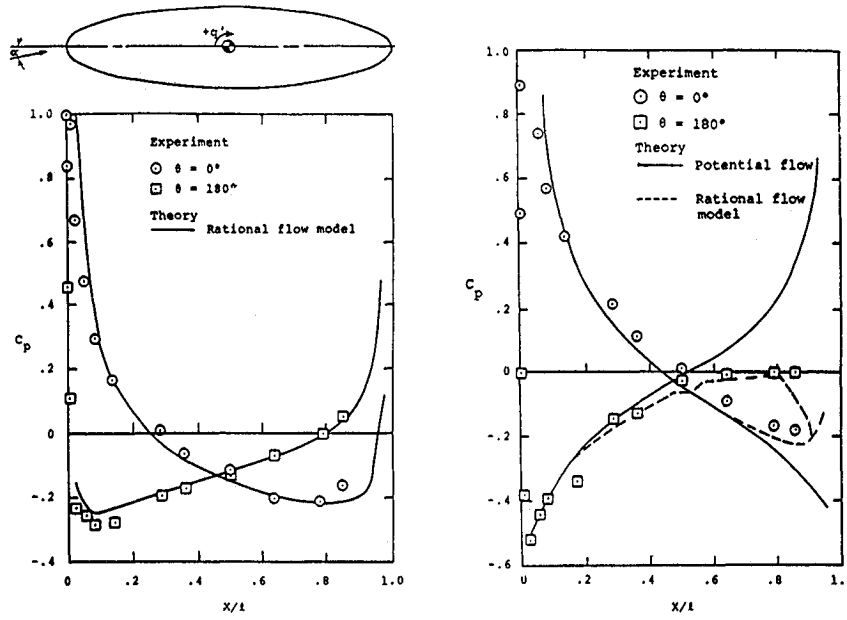

Fig. 8 Measured and predicted pressure distribution on a 4:1 ellipsoid body in a steady pitching maneuver.

a) $\alpha = 10$ deg, $q' = -0.0717$. b) $\alpha = 20$ deg, $q' = -0.0717$.

The predicted pressure distribution at $X/d = 7.5$ is compared with experiment in Fig. 6. The presence of the leeside wake has a significant affect on the pressure distribution and the prediction method successfully represents the vortex-induced effects. The potential results are shown as a dashed curve.

The total normal force coefficient is shown in Fig. 7. At lower angles of attack, the predicted results are in good agreement with the low Reynolds number experimental measurements; but at higher angles, it appears that the theory is in better agreement with the high Reynolds number results. This phenomenon is associated with the changing character of the separation on the missile in a transition region. Transition effects are not considered in the current investigation.

Steady Turning Maneuver

As discussed previously, a steady turning maneuver involves the missile at constant angles and constant angular rates and such a maneuver is represented experimentally on a rotating-arm apparatus. Measured pressure distributions on a 4:1 ellipsoid body of revolution in a steady turn are available for comparison.[16] Axial pressure distributions on the windward and leeward meridians are shown in Fig. 8 for $q' = -0.0717$ and two angles of attack ($\alpha = 10$ and 20 deg). The flow is such that the body is at positive angle of attack and is pitching nose downward such as to increase the local angle of attack at the nose and decrease the local angle at the base. In Fig. 8b, the effect of the separation vortex is shown to be significant in its effect on the leeside pressure.

Unsteady Maneuver

Unsteady force and moment data are not available for comparison purposes, but unsteady wake flow visualization results on an ogive-cylinder missile are available in Ref. 17.

A 3-caliber ogive nose and 7-caliber cylinder afterbody model was tested under forced pitching oscillation about its midpoint between $\alpha = 0$ and 30 deg, according to the schedule,

$$\alpha(t) = 15° + 15° \sin(2\pi ft + 3\pi/2) \qquad (33)$$

where $2\pi f = 1$. This results in a reduced frequency k of 0.2. Photographs of the vortex wake illustrate the vortex shedding characteristics of the model, and these unique experimental results provide heretofore unavailable detail concerning the complex flow phenomena associated with a pitching missile. The photographs are of a plane normal to the freestream velocity vector.

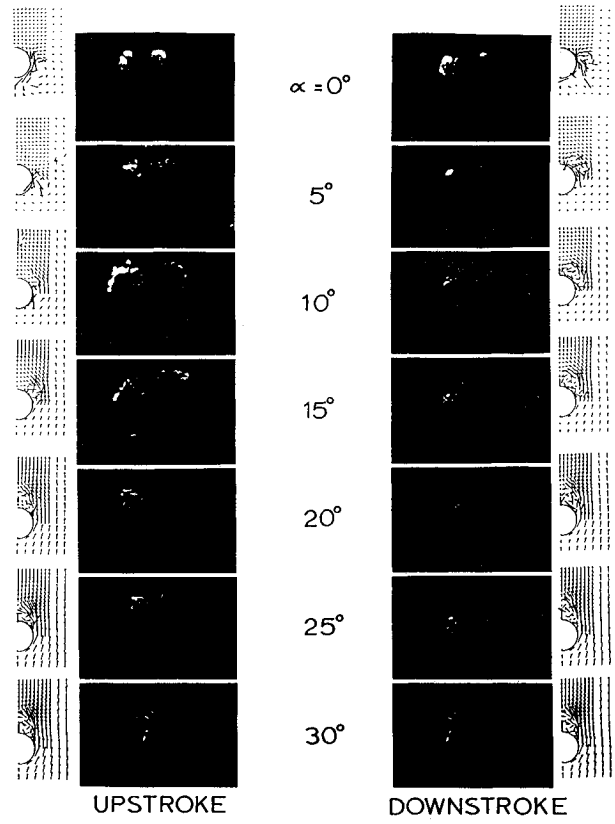

Fig. 9 Vortex wake at $X/\ell = 0.75$ on an ogive cylinder undergoing pitching motion, $k = 0.2$.

The prediction method was applied to the ogive-cylinder model and all of the results presented below were obtained over 1.5 complete cycles of motion to achieve a periodic

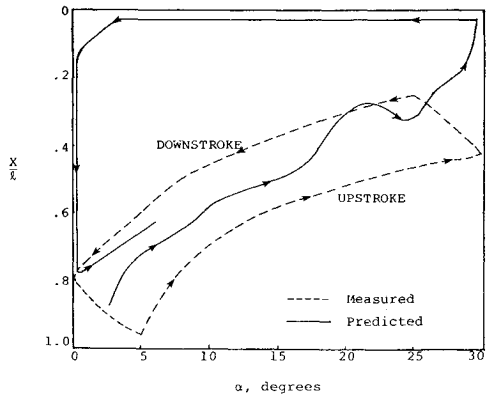

Fig. 10 Measured and predicted propagation of leeside separation of the ogive-cylinder missile undergoing pitching motion, $k=0.2$.

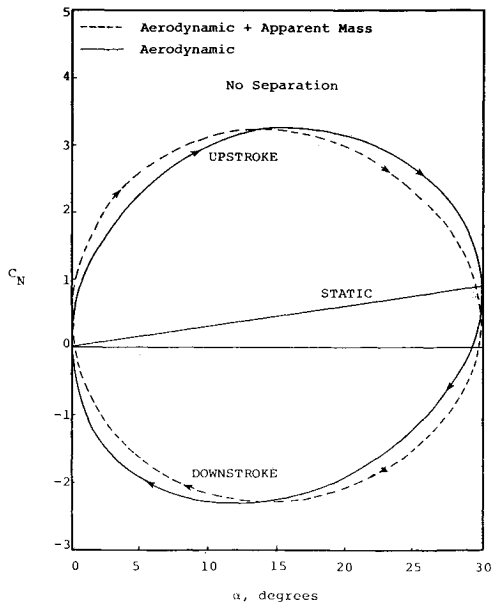

a) Linear result, no separation.

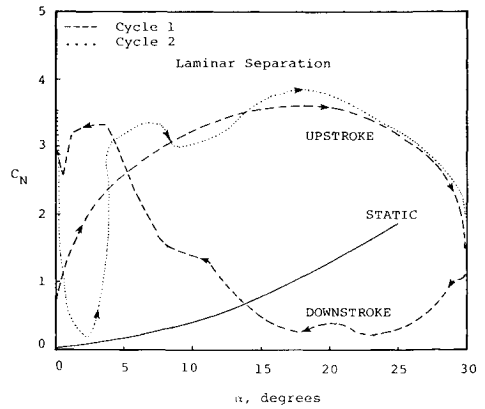

b) Nonlinear result, laminar separation.

Fig. 11 Predicted normal force coefficient on an ogive-cylinder missile undergoing pitching motion, $k=0.2$.

result. Because of the low Reynolds number of the tests, all vortex shedding is assumed to be laminar. The predicted velocity fields described below are in a plane normal to the missile axis.

Photographs of the wake at the $X/\ell=0.75$ station during one cycle are shown in Fig. 9, where it is assumed that $t=0$

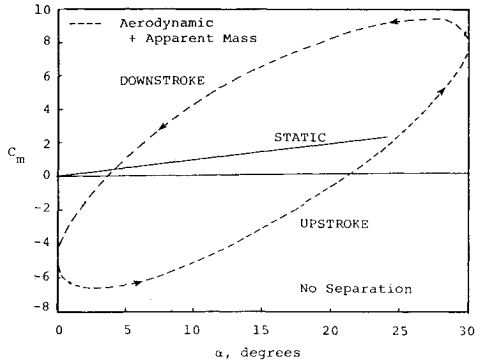

a) Linear result, no separation.

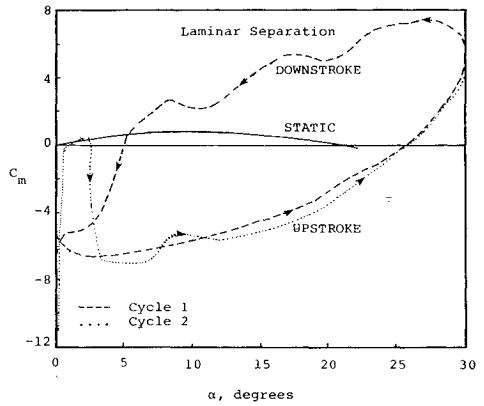

b) Nonlinear result, laminar separation.

Fig. 12 Predicted pitching moment coefficient on an ogive-cylinder missile undergoing pitching motion, $k=0.2$.

occurs at $\alpha=0$ deg on an upstroke. Therefore, the changing wake (time increasing) moves down the left-hand column of pictures to $\alpha=30$ deg and then moves up the right-hand column of pictures on the downstroke to return to $\alpha=0$ deg. Predicted velocity vectors on the right side of the model are shown at corresponding positions. Since the flow is symmetric, both sides of the model are not presented in the predicted figures. In Fig. 9, an attempt was made to align the vertical position of the model in the predictions with the position in the photographs. The velocity field, including vortex-induced effects, illustrates the extent of the wake better than a sketch of the discrete vortices.

Although only qualitative comparisons are possible, it appears that the predicted wake has many characteristics in common with the observed wake. For example, at $\alpha=0$ deg on the upstroke, the wake is concentrated near the side of the model. Note that a portion of this wake was actually shed from the nose on the downstroke of the previous cycle. As the model pitches upward, this station moves downward and the wake moves to the upper side of the missile. The strength of the wake at this station is also changing during the same period. As the model moves through the downstroke toward $\alpha=0$ deg on the right side of Fig. 9 the wake moves down to the side of the model; however, it appears in both the photographs and the predictions that the wake is more concentrated or tightly rolled up in this portion of the cycle. According to the predicted results, the strength of the vortex wake is stronger between $\alpha=10$ and 30 deg on the downstroke than it is at corresponding positions on the upstroke. The strongest vortices at this axial station occur at $\alpha=0$ deg.

An excellent discussion of the propagation of separation on a pitching missile is presented in Ref. 17. Based on flow visualization photographs, the observed propagation of separation is shown as the dashed curve (reproduced from

Ref. 17) in Fig. 10 for one complete pitching cycle. The predicted separation locations are shown as the solid curve. Arrows are used to denote the pitching direction. The predicted separation locations are defined as the axial stations at which separation first occurs. The predicted locations are always ahead of the measured locations because it is possible to detect much weaker vortices from the theory than are visible in the photographs. For example, on the downstroke, separation occurs at the nose of the missile for the entire stroke; however, these vortices often remain near the body surface until some distance downstream and they do not appear in the side-view photographs used to define the dashed curve.

Although force and moment data are not available for the pitching missile, predicted results are presented to illustrate the effect of vortex shedding on the nonlinear aerodynamic characteristics of the model. The predicted normal force coefficients on the missile are shown in Fig. 11 for both static and pitching conditions. The linear results with no vortex separation effects included are shown in Fig. 12a. The static condition is the result of the normal slender-body-theory. The dashed curve is the predicted total force on the missile, including both aerodynamic and apparent mass forces. The solid curve represents only the aerodynamic force.

The nonlinear effects of vortex shedding are shown in Fig. 12b, where the static results are similar to those shown in Fig. 7. For the pitching missile, the vortex-induced forces have a dominant effect on the total normal force coefficient. The first cycle, shown as a dashed curve, begins very smoothly on the upstroke and, because the vortex field has not had an opportunity to build up strength, the results up to $\alpha = 10$ deg are nearly identical to those shown on the upstroke without separation. The predicted normal force is slightly larger than the result without separation but on the downstroke where the strong vortex field developed on the upstroke is moving along the missile, the total normal force coefficient is very different from the unseparated results. The irregularities in the downstroke results in the first cycle are due to numerical difficulties in the vortex tracking. These difficulties carry over to the initial portion of the second cycle; however, they tend to smooth out and a periodic solution develops.

Predicted pitching moment coefficients are presented in Fig. 12 for the same flow conditions. The results are similar to those described above for normal force; however, the intensity of the vortex-induced effects are less because they are distributed over the entire missile.

The unsteady calculation described above required approximately 2.5 min per time step on a VAX 11/750 computer.

Conclusions

An engineering rational flow model to predict the aerodynamic characteristics and motion of a missile in unsteady maneuvers has been investigated. Comparison of measured and predicted static aerodynamic characteristics of a typical missile configuration verify that the principal features of the flow phenomena are well represented at moderate angles of attack above the linear aerodynamic range. The flow models were extended to include steady turning maneuvers and comparisons with experiment illustrated the capability of the method to predict the detailed aerodynamic characteristics under the influence of the leeside vortex field. Finally, the method was extended to consider unsteady flows in a time-dependent calculation of the aerodynamic characteristics of a missile in oscillating motion. Qualitative results indicate the flowfield prediction capability of the method.

The unsteady prediction method described in this paper illustrates an approach in which the nonlinear forces and moments are predicted for use in a direct calculation of the motion of a missile configuration. The method has application in the calculation of missile trajectories for configurations and flow conditions for which stability derivatives are unknown.

Acknowledgments

The preliminary study reported in this paper was funded under a Nielsen Engineering & Research, Inc., IR&D project. The photographs in Fig. 9 were provided by Dr. M. Gad-el-Hak.

References

[1]Mendenhall, M. R., Spangler, S. B., and Perkins, S. C. Jr., "Vortex Shedding from Circular and Noncircular Bodies at High Angles of Attack," AIAA Paper 79-0026, Jan. 1979.

[2]Mendenhall, M. R. and Perkins, S. C. Jr., "Prediction of Vortex Shedding from Circular and Noncircular Bodies in Supersonic Flow," NASA CR-3754, Jan. 1984.

[3]Mendenhall, M. R. and Lesieutre, D. J., "Prediction of Vortex Shedding from Circular and Noncircular Bodies in Subsonic Flow," NASA CR-4037, Jan. 1987.

[4]Perkins, S. C. Jr., Mendenhall, M. R., and Young, S. W., "Rational Flow Modeling of Submersible Vehicles, Vol. II, *RATFLO Program Manual*, Nielsen Engineering & Reseach Inc., Mountain View, CA, NEAR TR 265, Jan. 1982.

[5]Perkins, S. C. Jr. and Mendenhall, M. R., "Hydrodynamic Analysis of Submersible Vehicles Undergoing Large Unsteady Maneuvers," Vol. II-SUBFLO Program Manual, Nielsen Engineering & Research, Inc., Mountain View, CA, NEAR TR 341, April 1985.

[6]Marshall, F. J. and Deffenbaugh, F. D., "Separated Flow Over Bodies of Revolution Using an Unsteady Discrete-Vorticity Cross Wake, Part 1: Theory and Application," NASA CR-2414, June 1974.

[7]Wardlaw, A. B., "Multivortex Model of Asymmetric Shedding on Slender Bodies at High Angles of Attack," AIAA Paper 75-123, Jan. 1975.

[8]Deffenbaugh, F. D. and Koerner, W. G., "Asymmetric Wake Development and Associated Side Force on Missiles at High Angles of Attack," *Journal of Spacecraft and Rockets*, Vol. 14, March 1977, pp. 155-162.

[9]Goodwin, F. K., Nielsen, J. N., and Dillenius, M. F. E., "A Method for Predicting Three-Degree-of-Freedom Store Separation Trajectories at Speeds up to the Critical Speed," AFFDL-TR-79-4, March 1979.

[10]Cebeci, T., Mosinskis, G. J., and Smith, A. M. O., "Calculation of Viscous Drag and Turbulent Boundary-Layer Separation on Two-Dimensional and Axisymmetric Bodies in Incompressible Flow," McDonnell Douglas Corp., Rept. MDC JO 973-01 (Contract N00014-70-C-0099), Long Beach, CA, Nov. 1970.

[11]Stratford, B. S., "The Prediction of Separation of the Turbulent Boundary Layer," *Journal of Fluid Mechanics*, Vol. 5, 1959, pp. 1-16.

[12]Milne-Thomson, L. M., *Theoretical Hydrodynamics*, MacMillan, New York, 1968.

[13]Etkin, B., *Dynamics of Flight*, Wiley, New York, 1959.

[14]Lloyd, A.R.J.M., "Progress Towards a Rational Method of Predicting Submarine Maneuvers," *RINA International Symposium on Naval Submarines*, Vol. II, May 1983, Paper 21.

[15]Tinling, B. E. and Allen, C. Q., "An Investigation of the Normal-Force and Vortex-Wake Characteristics of an Ogive-Cylinder Body at Subsonic Speeds," NASA TN D-1297, April 1962.

[16]Jones, R., "The Distribution of Normal Pressures on a Prolate Spheroid, Royal Institute of Naval Architects, London, British Aeronautical Research Council, R&M 1061, Dec. 1925.

[17]Gad-el-Hak, M. and Ho C.-M., "Unsteady Flow Around an Ogive-Cylinder," AIAA Paper 86-0572, Jan. 1986.